Available online at www.sciencedirect.com
SCIENCE DIRECT
Journal of Catalysis 233 (2005) 453–463
JOURNAL OF CATALYSIS
www.elsevier.com/locate/jcat

Hydrogen production for fuel cell applications by ethanol partial oxidation on Pt/CeO_2 catalysts: the effect of the reaction conditions and reaction mechanism

L.V. Mattos, F.B. Noronha *

Instituto Nacional de Tecnologia (INT), Av. Venezuela 82, CEP 20081-312, Rio de Janeiro, Brazil

Received 9 February 2005; revised 12 April 2005; accepted 21 April 2005

Available online 21 June 2005

Abstract

This work studied the effect of reaction conditions and catalyst reducibility on the performance of the Pt/CeO_2 catalyst in the partial oxidation of ethanol. Oxygen storage capacity (OSC) measurements allowed evaluation of the oxygen transfer capacity of the catalysts. Metal dispersion was determined through cyclohexane dehydrogenation, a structure-insensitive reaction. Infrared spectroscopy of adsorbed ethanol, temperature-programmed desorption, and temperature-programmed surface reaction of ethanol was performed to establish the reaction mechanism. The low dispersion and low oxygen transfer capacity led to a decrease in both the activity and stability of Pt/CeO_2 catalysts on partial oxidation of ethanol. The higher amount of oxygen near the metal particles promotes the mechanism of carbon removal from the metallic surface, which takes place at the metal–support interfacial perimeter. Moreover, the increase in particle size decreases the metal–support interfacial area, reducing the effectiveness of the mechanism of carbon removal from the metallic surface. Furthermore, the results obtained on partial oxidation of ethanol showed that an increase in the residence time or reaction temperature increased the ethanol conversion and H_2 yield. Regarding selectivity for hydrocarbons and oxygenated products, the production of methane increased and the selectivity for acetaldehyde decreased as the residence time or reaction temperature was increased. At low conversions, the ethanol dehydrogenation dominates, forming acetaldehyde, whereas at high conversions the decomposition of ethanol is favored, producing CH_4, H_2, and CO. A reaction mechanism is proposed to explain the catalytic tests.

Keywords: H_2 production; Fuel cell; Partial oxidation of ethanol; Pt/CeO_2 catalysts

1. Introduction

Fuel cells are a promising technology for efficient and clean power for vehicles, residential units, offices, and commercial buildings [1]. Fuel cells require a source of hydrogen to produce electricity. However, hydrogen is difficult to transport and store. Fuel reforming offers a practical solution to the challenge of providing hydrogen for fuel cells onboard vehicles or for remote or stationary applications [2].

A variety of technologies, such as steam reforming (SR), partial oxidation (POX), and autothermal reforming (ATR) can be used to produce hydrogen from fuels like gasoline, diesel, LPG, methane, methanol, and ethanol [3]. The choice of fuel and fuel-processing technology depends on both the type of fuel cell and its application. For stationary power, natural gas is the preferred fuel, where it is available. However, the natural gas infrastructure does not extend to all areas. For automotive applications, gasoline and methanol are considered the two most promising fuels. Whereas gasoline has the advantage of a well-established infrastructure, hydrogen production from methanol occurs at lower temperatures.

* Corresponding author. Fax: +55-21-2123-1051.
E-mail address: fabiobel@int.gov.br (F.B. Noronha).

0021-9517/$ – see front matter
doi:10.1016/j.jcat.2005.04.022

Ethanol presents several advantages over other fuel sources. As a renewable fuel, ethanol used in fuel-cell vehicles or for stationary power plants generates far fewer greenhouse gases than conventional fuels such as gasoline or natural gas, since the CO_2 produced in the process is consumed in crop grows [4]. Furthermore, the infrastructure needed for ethanol production and distribution is already established in countries like Brazil and the United States, since ethanol is currently distributed and used as an octane enhancer or oxygenate blended with gasoline. According to automobile manufacturers, fuel infrastructure is one of the most critical issues in determining the choice of fuel for fuel-cell-powered vehicles [4]. Ethanol may also play an important role in distributed generation as a fuel source that is available in remote areas where natural gas infrastructure is not present.

Steam reforming of ethanol has been proposed for the production of hydrogen for fuel cells [5–17]. However, this process presents some disadvantages, such as formation of by-products and catalytic deactivation. Hence, the economic viability for the use of ethanol for this application depends on the development of new catalysts and determination of the appropriate reaction conditions.

Although several studies have been made on steam reforming of ethanol, information on partial oxidation is scarce in the literature. Partial oxidation systems have fast start-up and response times, which makes them attractive for following rapidly varying loads. Moreover, the POX reactor is more compact than a steam reformer, since it does not need the indirect addition of heat via a heat exchanger.

We have previously reported that Pt/CeO_2 catalysts provided good stability and activity to hydrogen production by partial oxidation of natural gas [18]. In this work, we study the effect of the reaction conditions and the catalyst reducibility on the performance of Pt/CeO_2 catalysts on the partial oxidation of ethanol. A reaction mechanism is proposed to explain the catalytic results.

2. Experimental

2.1. Catalyst preparation

Cerium oxide was prepared by two different methods: (i) calcination of cerium (IV) ammonium nitrate at 1073 K (CeO_2) and (ii) precipitation through the addition of ammonium hydroxide to an aqueous solution of cerium (IV) ammonium nitrate followed by calcination at 1073 K (CeO_2(prec)). Platinum was added to CeO_2 and CeO_2(prec) supports by incipient wetness impregnation with an aqueous solution of $H_2PtCl_6 \cdot 6H_2O$ and then dried at 393 K. The samples were calcined under air (50 cm^3/min) at 673 K for 2 h. Two catalysts, Pt/CeO_2 and Pt/CeO_2(prec), were obtained, and all catalysts contained 1.5 wt% platinum.

2.2. BET surface area

The BET surface areas of catalysts were measured with a Micromeritics ASAP 2000 analyzer by nitrogen adsorption at liquid nitrogen temperature.

2.3. Oxygen storage capacity

Oxygen storage capacity (OSC) measurements were carried out in a microreactor coupled to a quadrupole mass spectrometer (Omnistar, Balzers). Before OSC analysis, the samples were reduced under H_2 at 773 K for 1 h. Then the samples were cooled to 723 K and maintained at this temperature during the analysis. The mass spectrometer was used to measure the composition of the reactor effluent as a function of time while a 5% O_2/He mixture was passed through the catalyst. Oxygen consumption was calculated from the curve corresponding to $m/e = 32$.

2.4. Cyclohexane dehydrogenation

Platinum dispersion was estimated through cyclohexane dehydrogenation, a structure-insensitive reaction [19]. Since H_2 and CO spillover occurs over a CeO_2 support, metal dispersion could not be determined from the chemisorption of both gases [20]. To estimate the dispersion of the Pt/CeO_2 catalysts, a correlation between the rate of cyclohexane dehydrogenation and the metal dispersion measured by hydrogen chemisorption was established from Pt/Al_2O_3 catalysts with different metal particle sizes.

Cyclohexane dehydrogenation was performed in a fixed-bed reactor at atmospheric pressure. The catalysts were reduced at 773 K for 1 h, and the reaction was carried out at 543 K and WHSV = 170 h^{-1}. We fed the reactants to the reactor by bubbling H_2 through a saturator containing cyclohexane, with the intention of obtaining the desired H_2/HC ratio (13:1). The exit gases were analyzed with a gas chromatograph (Varian 300) equipped with a HP-Innowax column.

2.5. Infrared spectroscopy of adsorbed ethanol

Infrared spectroscopy analyses of adsorbed ethanol were performed with a Fourier transform infrared spectrometer (Magna 560 Nicolet). Before the analysis, the samples were reduced with H_2 at 773 K for 1 h. Then the samples were evacuated at the reduction temperature for 1 h and cooled to room temperature. The catalysts were exposed to 2 Torr of ethanol at room temperature for 1 h, and the spectra were collected after vacuum at 298, 373, 423, 473, 573, and 673 K.

2.6. Temperature-programmed desorption of ethanol

Temperature-programmed desorption (TPD) experiments with adsorbed ethanol were carried out in the same equip-

ment as already described for the OSC measurements. Before TPD analyses, the samples were reduced under flowing H_2 (30 cm^3/min) up to 773 K (5 K/min) and were maintained at that temperature for 1 h. After reduction, the system was purged with helium flow at the reduction temperature for 30 min and cooled to room temperature. The adsorption of ethanol was carried out at room temperature with pulses of an ethanol/He mixture, which we obtained by passing He through a saturator containing ethanol at 298 K. After adsorption, the catalyst was heated at a rate of 20 K/min rate up to 823 K in flowing helium (50 cm^3/min). The products were monitored with a quadrupole mass spectrometer (Balzers, Prisma). A Quadstar analytical system was used to record different signals of mass as a function of the temperature.

2.7. Temperature-programmed surface reaction

The temperature-programmed surface reaction (TPSR) was carried out by the same procedure as described for TPD analysis. All samples were reduced under flowing H_2 (30 cm^3/min) up to 773 K (5 K/min) and maintained at that temperature for 1 h. After reduction, the system was purged with helium at the reduction temperature for 30 min and cooled to room temperature. Ethanol was adsorbed at room temperature until the surface was saturated. After adsorption, the samples were purged with He and a 5% O_2/He mixture (50 cm^3/min) was passed as the temperature was raised at a 20 K/min rate to 823 K. The reaction products were monitored with a quadrupole mass spectrometer (Balzers, Prisma).

2.8. Reaction conditions

Ethanol partial oxidation was performed in a fixed-bed reactor at atmospheric pressure. Before reaction, the catalysts were reduced at 773 K for 1 h and then purged under N_2 at the same temperature for 30 min. The reaction was carried out on Pt/CeO_2 catalyst at different temperatures and for different residence times. On CeO_2 support and Pt/CeO_2(prec) catalyst, the ethanol partial oxidation was performed at 573 K and $W/Q = 0.16$ g s/cm^3 (W = weight of catalyst; Q = volumetric flow rate). To avoid hot spot formation and temperature gradients, catalyst samples were diluted with inert SiC (catalyst/SiC ratio = 1:3) to form a small catalyst bed (<5 mm in height). Furthermore, we fed the reactants to the reactor by bubbling air (30 cm^3/min) and N_2 (30 cm^3/min) through two saturators containing ethanol at 319 K, in order to obtain the desired ethanol/O_2 molar ratio (2.5:1) [21]. By working with this extremely diluted ethanol/oxygen mixture, we ensured the uniformity of the temperature of the catalyst bed.

The exit gases were analyzed with two gas chromatographs equipped with flame ionization and thermal conductivity detectors, respectively. This reaction was also carried out without catalyst (homogeneous reaction) at temperatures between 573 and 973 K. The ethanol conversion, hydrogen yield (hydrogen mol/consumed ethanol mol), CO_2/CO_x ratio, and selectivity for hydrocarbons and oxygenated products (selectivity for HC) reported for each run refer to measurements taken at steady conditions (at around 100 min time on stream, unless stated otherwise in the text). Since the hydrogen produced will be supplied to a PEM fuel cell, it is important to maximize the CO_2/CO_x ratio in order to favor the purification step. The CO_2/CO_x ratio and selectivity for HC (S_x) were calculated from

$$\frac{CO_2}{CO_x} = \frac{n_{CO_2}}{n_{CO_2} + n_{CO}} \times 100, \tag{1}$$

$$S_x = \frac{y_x}{y_M + y_{C_2} + y_{MOH} + y_{acetal} + y_{acetate}} \times 100, \tag{2}$$

where n_{CO_2} and n_{CO} are, respectively, CO_2 and CO in moles, and y_x is the weight fraction of the methane ($x = M$), ethane + ethene ($x = C_2$), methanol ($x = MOH$), acetaldehyde ($x =$ acetal), or ethyl acetate ($x =$ acetate).

3. Results

3.1. Characteristics of the samples

Table 1 lists BET surface areas obtained for the two catalysts. The Pt/CeO_2 catalyst showed a surface area slightly higher than that of Pt/CeO_2(prec). However, all samples exhibited low surface areas.

The oxygen uptake and dispersion calculated through cyclohexane dehydrogenation are also listed in Table 1. The oxygen storage capacity of the Pt/CeO_2 catalyst is significantly higher than that of the Pt/CeO_2(prec) catalyst. Pt/CeO_2 had higher dispersion than the Pt/CeO_2(prec) catalyst.

3.2. Infrared spectroscopy of adsorbed ethanol

Fig. 1 shows the IR spectra of adsorbed ethanol on the Pt/CeO_2 catalyst in the C–O stretching region (a, b, and c) and in the C–H stretching region (d). The IR spectrum after ethanol adsorption and evacuation at room temperature exhibits bands at 2978, 2933, 2118, 2087, 2054, 1687, 1600, 1574, 1547, 1525, 1425, 1400, 1340, 1315, 1265, 1120, 1082, 1056, 1040, and 1022 cm^{-1}. The bands at 2978 ($\nu_{as}(CH_3)$), 2933 ($\nu_{as}(CH_2)$), 1400 ($\delta_s(CH_3)$), 1082, and 1040 cm^{-1} (νCO) can be attributed to ethoxy species

Table 1
BET surface areas, O_2 uptakes measured at 723 K, specific rates of cyclohexane dehydrogenation and estimated metal dispersion

Catalyst	BET surface area (m^2/g_{cat})	O_2 uptake ($\mu mol/g_{cat}$)	Rate of cyclohexane dehydrogenation (mol/(g_{cat} h))	Dispersion (%)
Pt/CeO_2	14	194	0.191	48
Pt/CeO_2(prec)	9	18	0.062	15

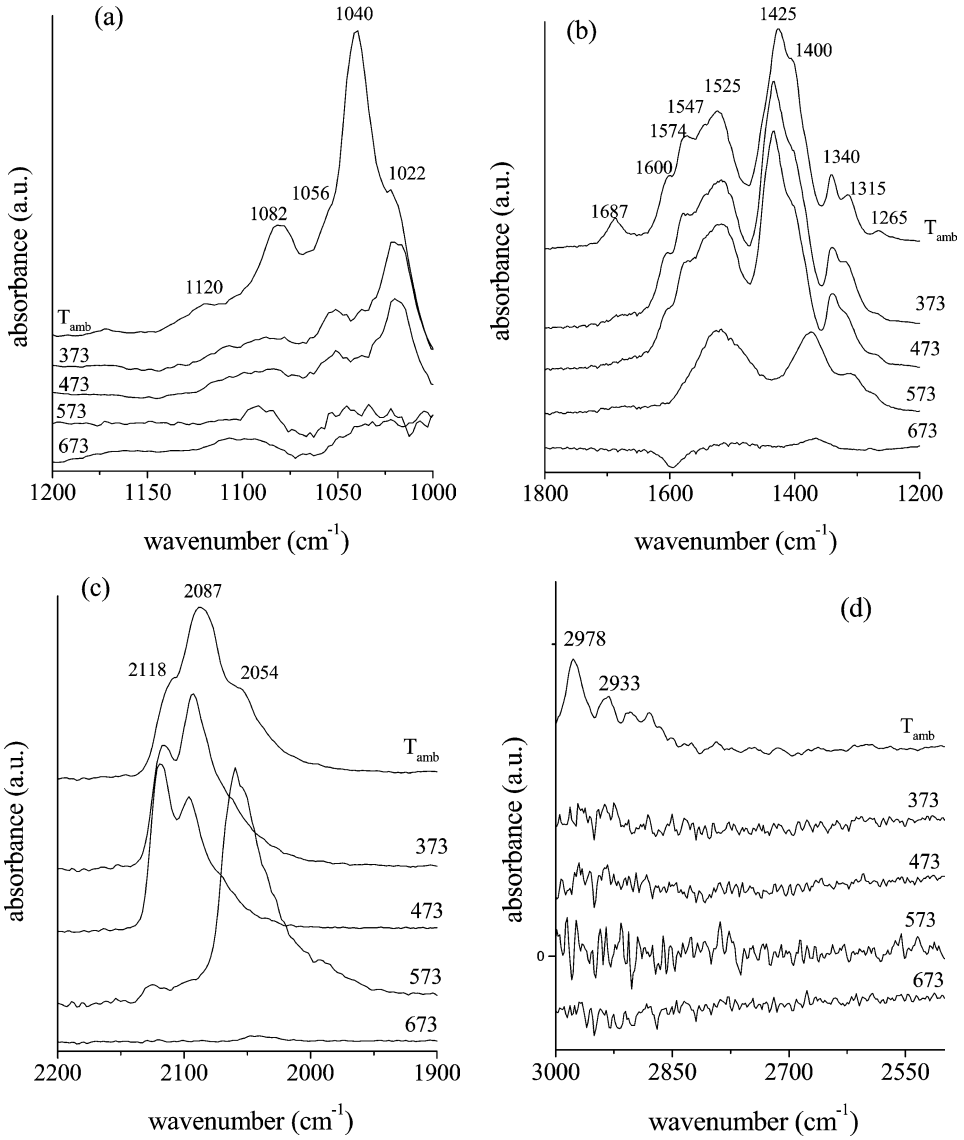

Fig. 1. Infrared spectra of the surface species formed by ethanol adsorption on reduced Pt/CeO_2 catalyst at different temperatures. (a–c) C–O stretching region; (d) C–H stretching region.

[22–24]. According to the literature, adsorption of alcohols such as methanol [25–28] and ethanol [22–24] on the surface of metal oxides occurs through an alkoxide species formed from the scission of the O–H bond.

The bands at 1600, 1574, 1547, 1425, 1340, and 1315 cm^{-1} indicate that a further oxidation of ethoxy species takes place, producing acetate and/or carbonate species. According to the assignments of vibrational modes for acetate [22–24] and carbonate [25,29–31] species from adsorption of ethanol, acetaldehyde, and acetic acid on CeO_2, Pd/CeO_2, and Pt/CeO_2, we can observe that it is very hard to distinguish one species from the other by its vibrational modes in the C–O stretching region. However, the shoulders at 1056 and 1022 cm^{-1} suggest that acetate species are formed, since characteristic bands related to carbonate species are not found in this region. These bands are due to the rocking modes of CH_3 [23]. Additional support for this assignment, obtained after the sample was heated at different temperatures, will be described later. But the presence of oxidation product intermediates on reduced Pt/CeO_2 even at room temperature is noticeable. It is also important to stress that no evidence of acetate or carbonate species was found on the reduced Pt/CeO_2 catalyst before ethanol adsorption.

After the samples were heated at 373 K, the bands corresponding to ethoxy species almost completely disappeared. On the other hand, the intensity of the bands associated with acetate species remained unchanged, even after evacuation at 473 K. However, heating to 573 K resulted in important changes in the spectra. All of the bands attributed to acetate species were no longer detected, whereas the bands characteristic of carbonate species (1523 and 1375 cm^{-1}) were now present (Fig. 1b). This result supports the idea of transformation of acetate species into carbonate species. It is worth noting that the appearance of the bands associated

with carbonate species in the CO stretching region is not accompanied by bands between 1200 and 1000 cm^{-1}. This confirms the previous proposal that acetate species were the only adsorbed oxidation intermediates formed at room temperature. At 673 K, no bands attributed to carbonate species are observed.

The bands observed between 2200 and 1650 cm^{-1} have been attributed to CO adsorption on Pt particles. FTIR of adsorbed CO on supported Pt catalysts has been used as an important tool for probing both electronic and particle morphology effects [32–35]. The IR bands can be divided into two regions. One region corresponds to the absorption bands between 2200 and 1900 cm^{-1}, which have been assigned to linearly adsorbed CO. In this region, the bands above 2050 cm^{-1} have been assigned to CO adsorbed on large Pt particles, whereas the bands below 2050 cm^{-1} correspond to linear CO adsorption on small Pt particles. The other region corresponds to the bands between 1900 and 1650 cm^{-1}, which are due to bridged or multicoordinated adsorbed CO [36–38]. In this work, the bands at 2087 and 2054 cm^{-1} could be attributed to CO adsorbed on Pt particles of different sizes.

The assignment of the band at 2118 cm^{-1} is controversial. This band has been related to the CO adsorption on Pt^{2+} [37] and on Pd^{2+} [39]. However, this band has also been observed in the IR spectra obtained in the absence of noble metal. Yee et al. [24] detected a band at 2122 cm^{-1} in the IR spectra for a reduced CeO_2 sample (before ethanol adsorption), which was formed from carbonate decomposition during reduction. They attributed this band to CO adsorbed on Ce^{3+} cations. Furthermore, this band appeared only on the unreduced and reduced Pt/CeO_2 catalyst after ethanol adsorption and heating at 523 K. The appearance of this band was followed by the formation of carbonate species. Therefore, in our work, the band at 2118 cm^{-1} could possibly be assigned to CO adsorption on Ce^{3+} cations, as previously reported [24].

Fig. 1c clearly shows that increasing the temperature to 473 K strongly decreased the absorbance of the bands of CO linearly adsorbed on Pt, whereas the band at 2118 cm^{-1} was practically not affected. Heating to 573 K led to the complete disappearance of the band at 2118 cm^{-1} and to a significant increase in the intensity of the band at 2054 cm^{-1}.

It is important to stress that the CO adsorbed at room temperature stems from the ethoxy species decomposition, in agreement with the TPD analysis, which will be presented next.

3.3. Temperature-programmed desorption of ethanol

TPD profiles of adsorbed ethanol on Pt/CeO_2 catalyst are shown in Fig. 2. Ethanol desorbed at one peak (422 K), whereas no acetaldehyde formation was detected. The Pt/CeO_2 catalyst exhibited the production of CO, CH_4, and H_2 at around 480 K, due probably to the decomposition of ethanol. A further formation of CO, CH_4, and H_2 and the appearance of CO_2 was observed at higher temperatures (above 550 K). No evidence of crotonaldehyde, acetone, or benzene formation was given by TPD analysis.

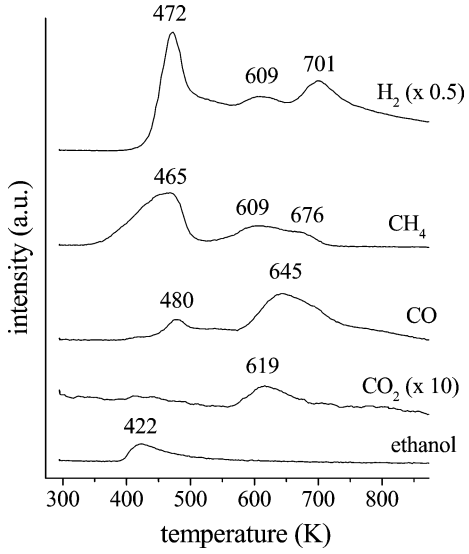

Fig. 2. TPD profile of ethanol adsorbed on Pt/CeO_2 catalyst.

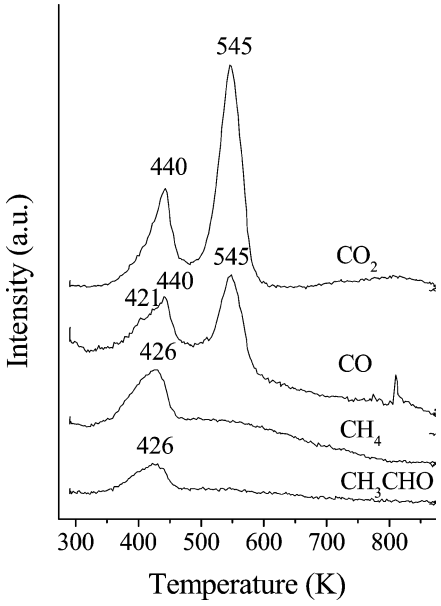

Fig. 3. Ethanol + oxygen TPSR profile on Pt/CeO_2 catalyst.

3.4. Temperature-programmed surface reaction

Fig. 3 shows the TPSR profiles for Pt/CeO_2 catalyst. Unlike the TPD results, acetaldehyde formation was observed at around 426 K with the simultaneous production of CH_4, CO, and CO_2. At 545 K, a large production of CO_2 and a small formation of methane occurred. Oxygen consumption was seen at 434 and 548 K.

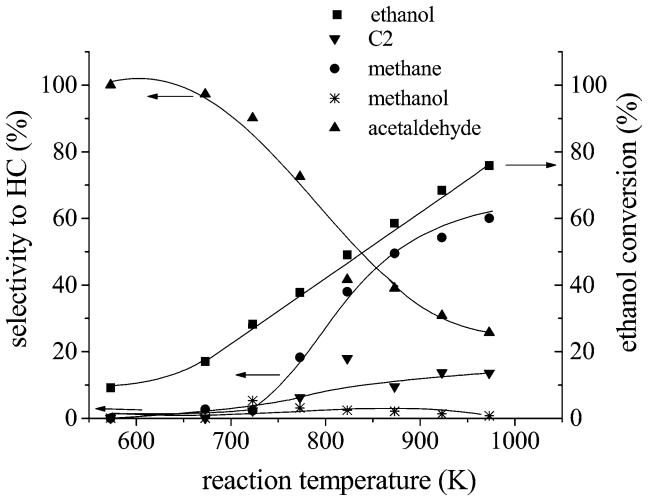

Fig. 4. Ethanol conversion and selectivity to HC on partial oxidation of ethanol versus reaction temperature in absence of catalysts (homogeneous reaction). Experimental conditions: flow rate = 60 cm^3/min and ethanol/O_2 = 2.5.

3.5. Partial oxidation of ethanol

3.5.1. Homogeneous reaction

Fig. 4 presents ethanol conversion and selectivity for HC versus reaction temperature obtained on the partial oxidation of ethanol in the absence of catalyst. The results showed that ethanol conversion became significant above 673 K, reaching values of 76% at 973 K. In terms of selectivity for HC, the main products obtained were acetaldehyde and methane. The increase in reaction temperature led to a decrease in acetaldehyde production and an increase in methane formation. Small amounts of C_2 (ethane and ethene) and methanol were also observed at temperatures higher than 673 K. To avoid such a homogeneous reaction, we studied the effect of the residence time on the performance of the Pt/CeO_2 catalysts at 573 K. The effect of reaction temperature on the activity, selectivity, and stability of the catalysts was evaluated between 473 and 673 K.

3.5.2. Stability

Ethanol conversion on the Pt/CeO_2 catalyst at three different temperatures and $W/Q = 0.16$ g s/cm^3 is described in Fig. 5. At 473 and 573 K, the catalyst was quite stable after a small initial transient period. When the reaction was run at 673 K, the ethanol conversion was complete. On the Pt/CeO_2(prec) catalyst, the ethanol conversion at 573 K strongly decreased with TOS. Therefore, the effect of reaction conditions was studied only for the Pt/CeO_2 catalyst, since this sample presented better stability for the partial oxidation of ethanol.

3.5.3. Effect of residence time and reaction temperature

At first, it is important to stress that the activity of pure ceria was negligible under the different reaction conditions studied. Fig. 6 presents the ethanol conversion and the H_2 yield as a function of residence time (W/Q) at 573 K on the Pt/CeO_2 catalyst. These results showed that increasing the residence time from 0.015 to 0.16 g s/cm^3 strongly increased the ethanol conversion and H_2 yield. However, this effect was less significant above 0.16 g s/cm^3. Similar results were obtained by Fatsikostas et al. [13] for steam reforming of ethanol on Ni/(La_2O_3/Al_2O_3) catalysts.

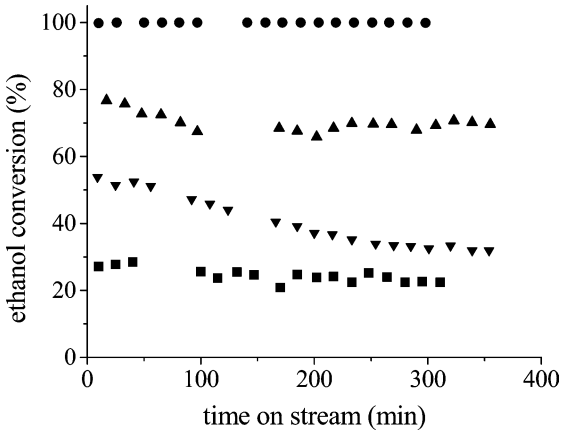

Fig. 5. Ethanol conversion on partial oxidation of ethanol for Pt/CeO_2 and Pt/CeO_2(prec) catalyst versus time on stream. Experimental conditions: Pt/CeO_2 catalyst: $T_{reaction}$ = 473 K (■); 573 K (▲); 673 K (●), and Pt/CeO_2(prec) catalyst: $T_{reaction}$ = 573 K (▼); $W/Q = 0.16$ g s/cm^3 and ethanol/O_2 = 2.5.

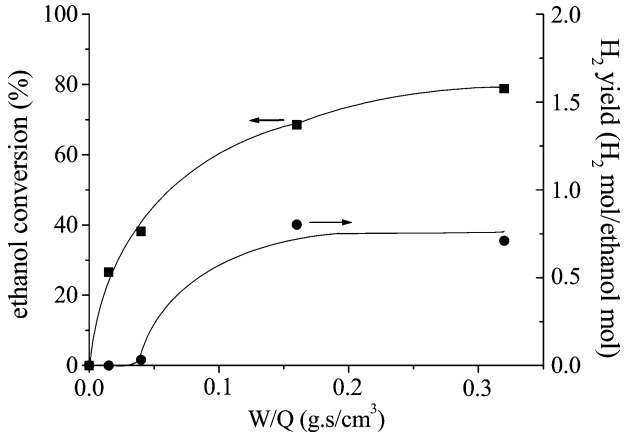

Fig. 6. Ethanol conversion and H_2 yield on partial oxidation of ethanol at 573 K as a function of residence time over Pt/CeO_2 catalyst.

Fig. 7 shows product selectivity and CO_2/CO_x ratio variations as a function of residence time. These results show that a strong decrease in the CO_2/CO_x ratio occurred when the residence time was increased from 0.015 to 0.32 g s/cm^3. Concerning the selectivity for HC, the main products obtained at 573 K were methane and acetaldehyde for all values of W/Q studied (Fig. 7). Furthermore, the selectivity for acetaldehyde decreased and the production of methane increased as the residence time was varied from 0.015 to 0.16 g s/cm^3. The formation of acetaldehyde and methane remained practically unchanged for residence times higher than 0.16 g s/cm^3. Liguras et al. [40] also observed greater amounts of acetaldehyde for low residence times on catalytic

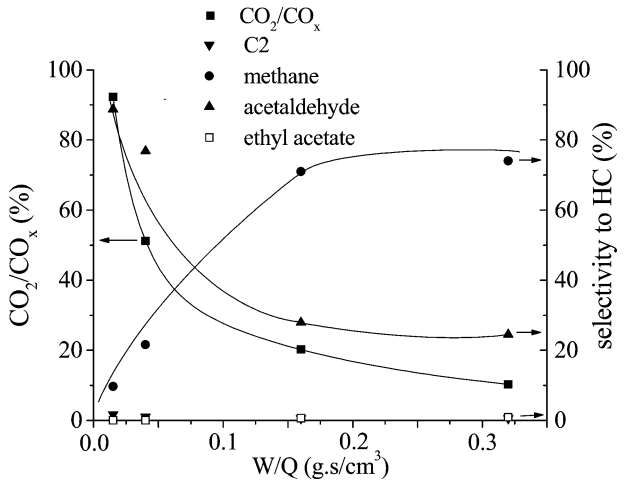

Fig. 7. CO_2/CO_x ratio and selectivity to HC on partial oxidation of ethanol at 573 K as a function of residence time over Pt/CeO_2 catalyst.

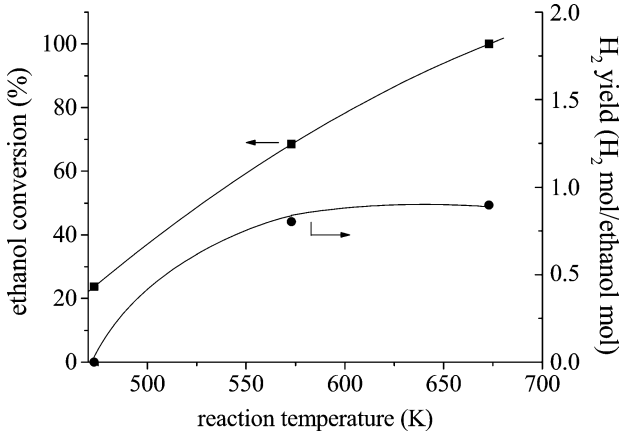

Fig. 8. Ethanol conversion and H_2 yield on partial oxidation of ethanol at $W/Q = 0.16\ \mathrm{g\,s/cm^3}$ as a function of reaction temperature over Pt/CeO_2 catalyst.

partial oxidation of ethanol over structured Ru catalysts. Fatsikostas et al. [13] studied the effect of contact time on the performance of $Ni/(La_2O_3/Al_2O_3)$ catalysts. The decrease in contact time was also followed by an increase in the selectivity for CH_3CHO, C_2H_4, and C_2H_6.

The ethanol conversion and the H_2 yield as a function of reaction temperature over Pt/CeO_2 catalyst at $W/Q = 0.16\ \mathrm{g\,s/cm^3}$ are shown in Fig. 8. The ethanol conversion strongly increased when the reaction temperature was raised from 473 to 673 K. The same behavior was observed for H_2 yield as the temperature was increased from 473 to 573 K. However, above 573 K, the enhancement of the H_2 yield was less pronounced.

Fig. 9 exhibits the CO_2/CO_x ratio and HC selectivity versus reaction temperature. The results obtained showed that the CO_2/CO_x ratio decreased as the reaction temperature was increased. This behavior is similar to the one observed, when the residence time was increased (Fig. 7).

At low temperature, the high CO_2/CO_x ratio is probably due to the oxidation of CO adsorbed on Pt particles,

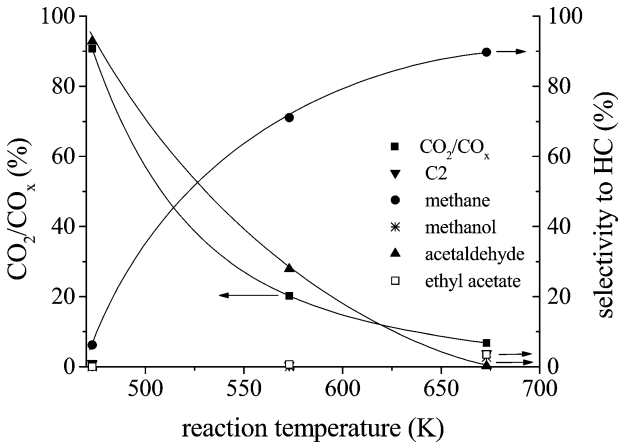

Fig. 9. CO_2/CO_x ratio and selectivity to HC on partial oxidation of ethanol at $W/Q = 0.16\ \mathrm{g\,s/cm^3}$ as a function of reaction temperature over Pt/CeO_2 catalyst.

which was detected by the IR measurements. This CO was produced through ethanol decomposition, in agreement with TPD analysis. At high temperature, the contribution of the ethanol decomposition reaction to the overall mechanism decreases, whereas the decomposition of carbonate species, producing CO_2, takes place. Since at this temperature oxygen was completely consumed, the CO_2 may replenish the oxygen vacancies of the support instead of being liberated to the gas phase. This can explain the decrease in the CO_2/CO ratio at high temperature.

Regarding selectivity for HC (Fig. 9): the main product obtained was acetaldehyde at 473 K. Only trace amounts of methane and C_2 were observed at this temperature. An increase in the reaction temperature from 473 to 573 K increased the selectivity for methane and decreased the acetaldehyde production. At 673 K, methane was the main product and acetaldehyde was no longer observed. Furthermore, small amounts of C_2, methanol, and ethyl acetate were detected at 673 K.

4. Discussion

4.1. Stability

One of the main issues in the production of H_2 from ethanol is the development of stable catalysts. Hence, the performance of CeO_2-supported Pt catalysts was evaluated as a function of TOS.

The strong deactivation of Pt/CeO_2(prec) catalyst could be attributed to carbon deposition or metal particle sintering. According to the literature, catalyst deactivation during ethanol steam reforming is mainly due to carbon deposition [13,16,17], which is strongly influenced by the nature of the support and the reaction conditions (reaction temperature; ethanol/water ratio). Information about the partial oxidation reaction is scarce. But carbon deposition has also been re-

ported on the partial oxidation of ethanol over Ru-based catalyst [40].

We have studied the performance of CeO_2- and Ce–ZrO_2-supported Pt catalysts on CO_2 reforming and partial oxidation of methane [41,42]. The results showed that the stability of these materials in both reactions is due to the occurrence of a carbon removal mechanism. According to this mechanism, carbon formed on a metal surface can partially reduce the oxide support near the metal particles, generating CO_x species and oxygen vacancies. In the absence of a reducible oxide, carbon will be deposited on the metal particle. The other path is the dissociation of CO_2 on the support followed by the formation of CO and O, which can reoxidize the support. Then CO_2 replenishes the oxygen vacancies and makes the support able to carry out the redox mechanism for continuous cleaning, promoting the carbon removal. The higher amount of oxygen vacancies near the metal particles promotes the mechanism of carbon removal from the metallic surface, which takes place at the metal–support interfacial perimeter. Furthermore, the increase in particle size decreases the metal–support interfacial area, reducing the effectiveness of the cleaning mechanism of metal particles [43].

In this work, the Pt/CeO_2 catalyst exhibited an oxygen storage capacity tenfold higher than that of the Pt/CeO_2(prec) catalyst. Furthermore, the Pt/CeO_2 catalyst also has higher dispersion than the Pt/CeO_2(prec) catalyst. It means that the mechanism of carbon removal from the metallic surface should not be effective on the Pt/CeO_2(prec) catalyst, leading to its deactivation. Therefore, in our work, the lower stability of the Pt/CeO_2(prec) catalyst on the partial oxidation of ethanol could be explained by its low dispersion and low oxygen transfer ability (Table 1).

Since the Pt/CeO_2 catalyst exhibited higher stability, the study of reaction mechanism was carried out on this catalyst.

4.2. Reaction mechanism

4.2.1. Ethanol adsorption

In this work, the IR analysis revealed that ethanol adsorbs as ethoxy species. However, a fraction of these ethoxy species are further oxidized to acetate species, even at room temperature. Idriss et al. [22] also observed the formation of ethoxy and acetates species after adsorption of acetaldehyde at room temperature on the surface of reduced ceria and ceria-supported Pd catalyts by IR spectroscopy. On the other hand, their studies of the adsorption of ethanol on CeO_2 [23], Pd/CeO_2 [23], Pt/CeO_2 [24], and Rh/CeO_2 [44] catalysts showed that ethanol adsorbed dissociatively to form ethoxy species on all surfaces studied. At this temperature, acetate species were observed only on unreduced CeO_2. According to the authors, the absence of acetate species on reduced CeO_2 and supported catalysts (unreduced and reduced) was due to partial reduction of the support.

The presence of acetate species on our Pt/CeO_2 catalysts even at room temperature is probably due to the redox properties of ceria. Several studies reported that cerium oxide has a very high oxygen exchange capacity [45,46]. This capacity is associated with the ability of cerium to act as an oxygen buffer through the storage/release of O_2 due to the Ce^{4+}/Ce^{3+} redox couple [46]. The OSC measurements of our Pt/CeO_2 catalysts correspond to around 13% Ce^{3+} on the support. Deeper reduction of CeO_2 samples has been reported after treatment at higher temperatures [47,48]. In fact, TPR analysis of this catalyst revealed the presence of two peaks at 443 and 1243 K [49]. The first one was due to the reduction of superficial cerium oxide promoted by platinum, and the second one corresponds to the reduction of bulk cerium oxide [50]. Hence, the partial reduction of the support took place on the periphery of the metal particle. This means that a large amount of mobile oxygen is still available after reduction at 773 K. Unfortunately, the group of Idriss and coworkers [23,24,44] measured neither the oxygen storage capacity of their catalysts nor the extension of support reduction. Thus it is difficult to compare the two works. The redox properties of their materials could possibly explain the differences observed. Nevertheless, it seems that their Pd/CeO_2, Pt/CeO_2, and Rh/CeO_2 catalysts have a lower capacity to exchange oxygen than the Pt/CeO_2 catalyst of this work.

Furthermore, the oxidation of ethoxy to acetate species should be followed by $Ce^{4+} \rightarrow Ce^{3+}$ reduction, since the IR experiments were carried out in the absence of oxygen. Therefore, the only oxygen source available to oxidize the ethoxy species to acetate stems from the support. This was also suggested by Finocchio et al. [26], who followed the thermal evolution of adsorbed methanol on pure ceria. According to the authors, the oxidation of on-top methoxy species on Ce^{4+} sites led to the production of formate species ($HCOO^-$) and H_2, which was accompanied by $Ce^{4+} \rightarrow Ce^{3+}$ reduction. H_2 evolution was detected by mass spectrometry.

The increase in temperature led to the complete disappearance of the bands corresponding to ethoxy species at around 373 K. On the other hand, the band intensities associated with acetate species remained unchanged. In fact, these bands were still present after evacuation at 473 K. Therefore, the disappearance of ethoxy species was not followed by the formation of acetate or carbonate species. In fact, TPD analysis revealed that the formation of methane begins at around 350 K, indicating that the adsorbed ethoxy species probably begins to decompose around this temperature. Several works have reported the appearance of CO, CH_4, and H_2 at the low-temperature region during TPD analysis of adsorbed ethanol, which was attributed to the decomposition of ethoxy species [23,51–53]. Cordi and Falconer [52] suggested that part of the ethanol adsorbed on alumina forms an ethoxy species that migrates to Pd sites, where decomposition take places. According to them, the α-carbon produced CO and the β-carbon formed CH_4 during ethanol decomposition. CO, CH_4, and H_2 were also produced at 495 K during a TPD experiment with ethanol on the Pd/Al_2O_3 cat-

alyst, because of the decomposition of ethanol on Pd [51]. Yee et al. [23,24,44] also observed the formation of CO, CH_4, and CO_2 during TPD analysis of ethanol on CeO_2 and Pd/CeO_2. However, these products were formed at high temperature (730 K) on the CeO_2 sample. In this region, the ethoxy species are no longer detected in the IR experiments with adsorbed ethanol on the support. This result confirmed that the decomposition of ethoxy species takes place on the metal particle.

In the literature, on Pd/CeO_2, Pt/CeO_2, and Rh/CeO_2 catalysts, a band at around 1700 cm^{-1} revealed the formation of acetaldehyde through the oxidative dehydrogenation of ethoxy species after the samples were heated [23,24,44]. Evidence of acetaldehyde formation was also provided by TPD analysis. Yee et al. [23,24,44] proposed that acetaldehyde species undergo decomposition to CH_4 and CO or produce carbonates, which are further oxidized to CO_2. On the Rh/CeO_2 catalyst, the C–C bond of ethanol is readily dissociated, producing adsorbed CO. Yee et al. [44] proposed that the formation of CH_4 and CO proceeded through CH_3 transfer to the surface and formation of CH_2O species, which is further decomposed to CO and hydrogen.

No evidence of acetaldehyde formation is observed on our Pt/CeO_2 catalysts by IR or TPD analysis. The same result was obtained by Yee et al. [23] when they studied the adsorption of ethanol on unreduced CeO_2. According to them, dehydrogenation of ethoxy species to acetaldehyde is followed by a very facile oxidation to acetate species due to the high amount of oxygen available. This could explain the absence of acetaldehyde species on the CeO_2 surface and agrees very well with the redox properties of our catalyst.

In this work, at higher temperatures, the bands related to acetate species vanished, suggesting that they underwent further oxidation, producing carbonate species, and decomposition to CO and CH_4, as observed in the TPD experiment (above 500 K). The decomposition of carbonate species is probably responsible for the CO_2 formation at 619 K (Fig. 2). However, the amount of CO_2 formed is low. In fact, we have previously demonstrated that CO_2 can replenish the oxygen vacancies of the support, releasing CO as a product [54,55]. This agrees very well with the large CO evolution detected at high temperature on our TPD analysis. Formation of CO, CO_2, and H_2 at high temperatures has also been observed over alumina-supported catalyts [51,52]. According to Cordi and Falconer [52], it might be due to the decomposition of a more stable carbon species formed during ethanol decomposition at lower temperatures. They further suggested that acetaldehyde or acetic acid could be the precursor for this more stable carbon species. Infrared studies of adsorbed ethanol on Pd/Al_2O_3 and $Pd–Mo/Al_2O_3$ catalysts showed the formation of acetate species as the temperature was raised from 523 to 573 K [51]. According to Baldanza et al. [51], ethanol is dehydrogenated on Pd sites to form acetaldehyde and more stable acetate species. These species remain adsorbed and are the precursors for the CO, H_2, and CO_2 production observed at high temperature. When compared with ceria support, acetate species on alumina-supported catalysts are formed at higher temperatures because of the lower ability to release/store oxygen of this support. Furthermore, in this case, an important desorption of CO_2 at high temperature is observed because alumina does not have oxygen vacancies as cerium oxide.

Finally, the large H_2 production detected on the TPD profile at high temperature could be attributed to the desorption of previously formed hydrogen. We have carried out TPD studies of H_2 adsorbed on this Pt/CeO_2 catalyst [49], and the profile exhibited two peaks at 353 and 613 K. The low-temperature peak was assigned to the hydrogen desorption from the metal surface, whereas the other one was due to the hydrogen from the support, which was previously transferred from the metal to the support (spillover) [56]. In this work, the hydrogen production peak agrees very well with our previous results.

4.2.2. *Ethanol + oxygen reaction*

A comparison between the TPD profile of adsorbed ethanol and the TPSR results reveals some important differences. In the presence of oxygen (Fig. 3), not only does the decomposition of ethoxy species take place, but also the oxidative dehydrogenation to acetaldehyde. It seems that ethoxy species formed on the surface underwent oxidation by the oxygen from the feed simultaneously with its decomposition. This explains the simultaneous observation of acetaldehyde desorption and methane formation. In addition, the decomposition of ethoxy species to methane was not followed by H_2 and CO production on the TPSR analysis, which is due to its further oxidation to H_2O and CO_2. At high temperature, the acetate species formed at room temperature and those that remained unreacted are oxidized, producing more CO_2.

In the literature, there are controversial results concerning the participation of acetate species as an intermediate that takes part in the reaction mechanism.

Sheng et al. [57] observed that the increase in reaction temperature from 473 to 673 K led to a decrease in acetaldehyde production and an increase in methane formation on partial oxidation of ethanol over $Rh–Pt/CeO_2$ catalysts. According to them, ethanol adsorbs as ethoxy species that further react to form acetaldehyde. They suggested that acetaldehyde decomposes, producing CO and CH_4 at high temperatures, but acetate formation was not proposed. In fact, they only carried out TPD and IR analysis in the absence of oxygen, which may not completely represent all of the reactions involved.

According to de Mello et al. [53], who studied the NO reduction with ethanol on Pd/Al_2O_3 catalyst by temperature-programmed analysis, acetaldehyde formation is an important step in the creation of more stable acetate species. According to the proposed mechanism, as soon as dehydrogenation of ethanol occurs, the acetaldehyde intermediate readily leads to the acetate species, which immediately react with the adsorbed NO. Similar observations were made

by other authors in their investigation of ethanol oxidation reactions. Nagal and Gonzalez [58] studied the oxidation of ethanol and acetaldehyde on Pt/SiO_2 catalysts by in situ infrared analyses. Based on their observations, they proposed a reaction mechanism in which the dehydrogenation of an adsorbed ethoxy species would be the limiting step. These dehydrogenated species could then be oxidized to form intermediate acetate species that would react, yielding CO_2.

Based on these observations, the following reaction mechanism could be proposed to explain the partial oxidation of ethanol on Pt/CeO_2 catalysts.

At first, ethanol adsorbs on ceria, producing an ethoxy species:

$$CH_3CH_2OH(g) + Ce^{4+} \rightarrow CH_3CH_2O\text{–}Ce^{4+} + (1/2)H_2. \quad (4)$$

In the absence of oxygen in the feed, a fraction of the ethoxy species can be dehydrogenated and immediately reacts with oxygen from the support to form acetate species,

$$CH_3CH_2O\text{–}Ce^{4+} \rightarrow CH_3CHO\text{–}Ce^{4+} + (1/2)H_2, \quad (5)$$

$$CH_3CHO\text{–}Ce^{4+} + Ce^{4+}\text{–}O^{2-} \rightarrow Ce^{3+}\text{–}CH_3COO\text{–}Ce^{3+} + (1/2)H_2, \quad (6)$$

which is followed by the $Ce^{4+} \rightarrow Ce^{3+}$ reduction.

When the temperature is increased, another fraction of the ethoxy species can migrate to the metal particle and is decomposed, forming CH_4, H_2, and CO:

$$CH_3CH_2O\text{–}Pd \rightarrow CH_4 + CO + (1/2)H_2 + Pd. \quad (7)$$

At high temperature, the acetate species previously formed can be decomposed to CH_4 and CO and/or oxidized to CO_2 via carbonate species:

$$OH^- + CH_3COO^- \rightarrow CH_4 + CO + O^{2-}, \quad (8)$$

$$OH^- + CH_3COO^- \rightarrow CH_4 + {CO_3}^{2-}, \quad (9)$$

$${CO_3}^{2-} \rightarrow O^{2-} + CO_2. \quad (10)$$

Under an oxygen atmosphere, the intermediate dehydrogenated species formed as indicated above in Eq. (5) may desorb as acetaldehyde while the Ce^{4+}–O site is recovered (Eq. (11)). This is indicated by a comparison of the TPD results, where no acetaldehyde was observed, with the TPSR results, where acetaldehyde formation occurred. The other steps are similar to the ones described in the absence of oxygen in the feed. This fully agrees with the increase in methane production followed by the decrease in acetaldehyde formation that occurs as the reaction temperature is increased (Fig. 7):

$$CH_3CHO\text{–}Ce^{4+} + (1/2)O_2(g) \rightarrow CH_3CHO(g) + Ce^{4+}\text{–}O. \quad (11)$$

5. Conclusions

The results obtained in this work show that the Pt/CeO_2 catalyst can perform the partial oxidation of ethanol with good stability and activity at 573 K. Furthermore, at higher temperatures and higher residence times, the only by-product detected on this catalyst is methane, which is not considered a contaminant of fuel cells. Higher methane levels are acceptable in the fuel-cell systems, because methane is combusted as a fuel in the reformer.

In addition, a large metal particle size and the low reducibility of the support led to a decrease in the activity and the stability of the Pt/CeO_2 catalysts. The presence of a large particle size decreases the metal–support interfacial area, reducing the effectiveness of the mechanism of carbon removal from the metallic surface, which takes place at the metal–support interfacial perimeter.

A reaction mechanism was proposed to explain the partial oxidation of ethanol on Pt/CeO_2 catalysts based on the IR, TPD, and TPSR experiments. According to this mechanism, adsorption of ethanol on the support gives rise to ethoxy species. In the absence of oxygen in the feed, a fraction of the ethoxy species can be dehydrogenated, which readily reacts with oxygen from the support, producing acetate species and Ce^{3+}. The extension of the oxidation reaction depends on the amount of oxygen from the support, whose degree of reduction is a function of the metal and pretreatment conditions. With increased temperature, another fraction of the ethoxy species migrates to the metal particle and is decomposed, forming CH_4, H_2, and CO. Furthermore, the acetate species previously formed can be decomposed to CH_4 and CO and/or oxidized to CO_2 via carbonate species. Under an oxygen atmosphere, the intermediate dehydrogenated species formed may desorb as acetaldehyde.

Acknowledgments

The authors wish to acknowledge the financial support of the CNPq and CNPq/Edital Universal program (476954/01-0).

References

[1] J. Strakey, M. Williams, 2003 Fuel Cell Seminar, Miami Beach, FL, 2003, p. 756.
[2] L. Carrette, K.A. Friedrich, U. Stimming, Fuel Cells 1 (2001) 5.
[3] J.R. Rostrup-Nielsen, Phys. Chem. Chem. Phys. 3 (2001) 283.
[4] J. Bentley, R. Derby, Ethanol and Fuel Cells: Converging Paths of Opportunity, report for the Renewable Fuels Association, 2002.
[5] N. Takezawa, N. Iwasa, Catal. Today 36 (1997) 45.
[6] F.J. Marino, E.G. Cerrela, S. Duhalde, M. Jobbagy, M.A. Laborde, Int. J. Hydrogen Energy 12 (1998) 1095.
[7] F.J. Marino, M. Boveri, G. Baronetti, M. Laborde, Int. J. Hydrogen Energy 26 (2001) 665.
[8] E.Y. Garcia, M.A. Laborde, Int. J. Hydrogen Energy 16 (1991) 307.
[9] S. Freni, N. Mondello, S. Cavallaro, G. Cacciola, V.N. Parmon, V.A. Sobyanin, React. Kinet. Catal. Lett. 71 (2000) 143.
[10] V.V. Galvita, G.L. Semin, V.D. Belyaev, V.A. Semikolenov, P. Tsiakaras, V.A. Sobyanin, Appl. Catal. A: Gen. 220 (2001) 123.
[11] A.N. Fatsikostas, D.I. Kondarides, X.E. Verykios, Chem. Commun. 851 (2001).

[12] S. Cavallaro, N. Mondello, S. Freni, J. Power Sources 102 (2001) 198.
[13] A.N. Fatsikostas, D.I. Kondarides, X.E. Verykios, Catal. Today 75 (2002) 145.
[14] J.P. Breen, R. Burch, H.M. Coleman, Appl. Catal. B: Environ. 39 (2002) 65.
[15] J. Llorca, N. Homs, J. Sales, P.R. de la Piscina, J. Catal. 209 (2002) 306.
[16] M.A. Goula, S.K. Kontou, P.E. Tsiakaras, Appl. Catal. B: Environ. 49 (2004) 135.
[17] A.N. Fatsikostas, X.E. Verykios, J. Catal. 225 (2004) 439.
[18] F.B. Passos, E.R. Oliveira, C.E.E.L. Rego, L.V. Mattos, F.B. Noronha, Fuel Chem. Div. Prep. 48 (1) (2003) 325.
[19] M. Boudart, Adv. Catal. 20 (1969) 153.
[20] P. Pantu, G.R. Gavalas, Appl. Catal. A 223 (2002) 253.
[21] S. Cavallaro, V. Chiodo, A. Vita, S. Freni, J. Power Sources 99 (2003) 10.
[22] H. Idriss, C. Diagne, J.P. Hindermann, A. Kiennemann, M.A. Barteau, J. Catal. 155 (1995) 219.
[23] A. Yee, S.J. Morrison, H. Idriss, J. Catal. 186 (1999) 279.
[24] A. Yee, S.J. Morrison, H. Idriss, J. Catal. 191 (2000) 30.
[25] C. Binet, M. Daturi, J.C. Lavalley, Catal. Today 50 (1999) 207.
[26] E. Finocchio, M. Daturi, C. Binet, J.C. Lavalley, G. Blanchard, Catal. Today 52 (1999) 53.
[27] A. Badri, C. Binet, J.C. Lavalley, J. Chem. Soc. Faraday Trans. 93 (1997) 1159.
[28] M. Badlani, I. Wachs, Catal. Lett. 75 (2001) 137.
[29] R. Frety, P.J. Levy, V. Perrichon, V. Pitchon, M. Primet, E. Rogemond, N. Essayem, M. Chevrier, C. Gauthier, F. Mathis, Proceedings of 3rd Congress on Catalysts and Automotive Pollution Control, CAPOC III, vol. 2, 1994, p. 265.
[30] C. Li, Y. Sakata, T. Arai, K. Domen, K. Maruya, T. Onishi, J. Chem. Soc. Faraday Trans. I 85 (1989) 1451.
[31] C. Binet, A. Jadi, J.C. Lavalley, J. Chim. Phys. 89 (1992) 1779.
[32] C. Besoukhavnova, J. Guidot, D. Barthomeuf, M. Breysse, J.R. Bernard, J. Chem. Soc. Faraday Trans. 1 77 (1981) 1595.
[33] B.L. Mojet, J.T. Miller, D.C. Koningsberger, J. Phys. Chem. 103 (1999) 2724.
[34] G. Jacobs, F.G. Ghadiali, A. Pisanu, A. Borgna, W.E. Alvarez, D.E. Resasco, Appl. Catal. 188 (1999) 79.
[35] A.Y. Stakheev, E.S. Shpiro, N.I. Jaeger, G. Schulz-Ekloff, Catal. Lett. 32 (1995) 147.
[36] P.V. Menacherry, G.L. Haller, J. Catal. 177 (1998) 175.
[37] H. Bischoff, N.I. Jaeger, G. Schulz-Ekloff, L. Kubelkova, J. Mol. Catal. 80 (1993) 95.
[38] M. Primet, J. Catal. 88 (1984) 273.
[39] S. Yang, A. Maroto-Valiente, M. Benito-Gonzalez, I. Rodriguez-Ramos, A. Guerrero-Ruiz, Appl. Catal. B 28 (2000) 223.
[40] D.K. Liguras, K. Goudani, X.E. Verykios, Int. J. Hydrogen Energy 29 (2004) 419.
[41] L.V. Mattos, E.R. de Oliveira, P.D. Resende, F.B. Noronha, F.B. Passos, Catal. Today 77 (2002) 245.
[42] L.V. Mattos, E.R. de Oliveira, D.E. Resasco, F.B. Passos, F.B. Noronha, Fuel Process. Technol. 83 (2003) 146.
[43] S.M. Stagg-Williams, F.B. Noronha, G. Fendley, D.E. Resasco, J. Catal. 194 (2000) 240.
[44] A. Yee, S.J. Morrison, H. Idriss, Catal. Today 63 (2000) 327.
[45] J. Kaspar, P. Fornasiero, M. Graziani, Catal. Today 50 (1999) 285.
[46] M.H. Yao, R.J. Baird, F.W. Kunz, T.E. Hoost, J. Catal. 166 (1997) 67.
[47] F. Fally, V. Perrichon, H. Vidal, J. Kaspar, G. Blanco, J.M. Pintado, S. Bernal, G. Colon, M. Daturi, J.C. Lavalley, Catal. Today 59 (2000) 373.
[48] H. Vidal, J. Kaspar, M. Pijolat, G. Colon, S. Bernal, A. Cordon, V. Perrichon, F. Fally, Appl. Catal. B: Environ. 27 (2000) 49.
[49] E.R. de Oliveira, L.V. Mattos, F.B. Noronha, F.B. Passos, Proceedings of 11th Brazilian Congress on Catalysis, vol. 1, 2001, p. 529.
[50] H.C. Yao, Y.F. Yao, J. Catal. 86 (1984) 254.
[51] M.A.S. Baldanza, L.F. de Mello, A. Vannice, F.B. Noronha, M. Schmal, J. Catal. 192 (2000) 64.
[52] E.M. Cordi, J.L. Falconer, J. Catal. 162 (1996) 104.
[53] L.F. de Mello, F.B. Noronha, M. Schmal, J. Catal. 220 (2003) 358.
[54] F.B. Noronha, G. Fendley, R.R. Soares, W.E. Alvarez, D.E. Resasco, Chem. Eng. J. 11 (2001) 3775.
[55] S.M. Stagg-Williams, F.B. Noronha, G. Fendley, D.E. Resasco, J. Catal. 194 (2000) 240.
[56] S. Bernal, J.J. Calvino, M.A. Cauqui, J.M. Gatica, C. Larese, J.A. Perez Ornil, J.M. Pintado, Catal. Today 50 (1999) 175.
[57] P.-Y. Sheng, A. Yee, G.A. Bowmaker, H. Idriss, J. Catal. 208 (2002) 393.
[58] M. Nagal, R.D. Gonzalez, Ind. Eng. Chem. Prod. Res. Dev. 24 (1985) 525.